

Enhancement and Segmentation of Scar Color Images after a Scoliosis Surgery

Thomas Hurtut^{1,2}, Farida Cheriet^{1,2}, Julie Joncas², and Jean Dansereau^{1,2}

¹ Ecole Polytechnique,

P.O. Box 6079, Station Centre-Ville, Montreal, H3C 3A7, Canada
{thomas.hurtut, farida.cheriet, jean.dansereau}@polymtl.ca

² Hopital St-Justine,

3175 Chemin de la Cote St-Catherine, Montreal, H3T 1C5, Canada
julie@justine.umontreal.ca

Abstract. In this paper, a color-based segmentation scheme applied to dermatoscopic scar images is proposed. The image is first preprocessed via a partial differential equations (PDE)-based filter which combines in the RGB color space coherent anisotropic diffusion and shock filters. Then the scar image is segmented using a segmentation algorithm based on color distributions. A post-processing algorithm was further developed to extract the scar contour, based on spline interpolations, smoothed with the generalized-cross validation method. Experiments on real patient images show the performance of the proposed method.

1 Introduction

Scoliosis is a complex 3D deformity of the spine, rib cage and pelvis. About one of a thousand adolescent diagnosed with scoliosis require surgery, which involves a long scar on the back surface of the patient trunk. To avoid some clinical and esthetic complications due to the length of the scar and its position on the back, a follow-up is necessary. This follow-up should give information such as the area of the scar, its depth and its contrast based on color information. These clinical indices are intended to support the dermatologist in the supervised quantification of diagnosis features, during the time evolution of the scar.

Several segmentation schemes applied to color images of pigmented skin lesions were proposed. They deal with a few problems that are scar's - noise and small structural components elimination. A method based on two dimensional color histogram and clustering was presented in [1] to extract skin lesions contours. A color geodesic active contours method was presented in [2] to solve the same problem with hair. They both exploit the high contrast and the regular size of skin lesions. Unfortunately, scars are too thin and scattered to be detected either by active contour or by histogram procedures.

The goal of this paper was to develop a system that automatically extract the borders of such scars, using images captured with an active vision system designed to acquire 3D textured surface views of the trunk. Such an automatic

system allows precise follow-up, and make databases on scars evolution building-up possible. Such databases allow objective comparison between different wound closing techniques, industrial tools, and wire involved in plastic surgery procedures.

2 The proposed method

2.1 Image acquisition procedure

When a surgery is prescribed, the patient is scanned before and after the surgery³ for different applications besides the one described here. The system is composed of three 3D monoscopic cameras⁴ which work in visible light. A view of the system is given on Fig. 1. Only the color texture of the back of the patient is used in this paper since the scar is always in the back.



Fig. 1. Active vision image acquisition system [3]

Due to the calibration of the system, and the need to capture the whole scar in one shot, the camera is placed quite far from the patient. Hence the resolution of the scar is quite small. Its contrast and level noise compared to the width of the scar is rather high too. Consequently, an important preprocessing step is necessary to enhance the contrast and denoise the image.

2.2 Preprocessing Algorithm

In order to eliminate small structure components and noise, a PDE-based filter was designed. This filter is composed of an anisotropic diffusion filter and a shock filter, both using a measure of local coherence on color space.

³ this system is used at St-Justine Hospital, Montreal, Canada

⁴ 3D Inspeck cameras, manufactured in Quebec Canada

Coherent anisotropic diffusion In opposition to the classic anisotropic circular diffusion of Perona and Malik [4], coherent diffusion allows elliptic diffusion. The coherent diffusion model takes the form :

$$\partial_t u = \text{div}[D\nabla u] \quad (1)$$

where $D \in \mathbb{R}^{2 \times 2}$ and ∂_t is the partial derivative on t . D defines the diffusion along the direction and the normal to ∇u . There were many works on different ways to define the diffusivity matrix D for since. Here the regularized structure tensor matrix $J_\rho(\nabla u_\sigma)$ is used ([5]):

$$J_\rho(\nabla u_\sigma) = \mathcal{N}_\rho * (\nabla u_\sigma \otimes \nabla u_\sigma) \quad (2)$$

where u_σ is the regularized image of u by convolving with a Gaussian $\mathcal{N}_\sigma(x, y) = (2\pi\sigma^2)^{-1} \exp(-\frac{x^2+y^2}{2\sigma^2})$, and ρ is the integration scale. The convolution with \mathcal{N}_ρ is done component-wise mainly to average a feature over a known neighborhood and over which the orientation information is average. In (2) a measure of ∇u on scalar images is used, but it can be generalized to color images ([6]):

$$J_\rho(\nabla \vec{u}_\sigma) = \sum_{i=1}^3 J_\rho(\nabla u_{i,\sigma}) \quad (3)$$

where $u_{i,\sigma}$ denotes the i th channel on RGB space. Since this matrix is symmetric positive semi-definite, using eigenvalue decomposition, the formulation in (2) can be put as :

$$J_\rho(\nabla \vec{u}_\sigma) = (w_1 | w_2) \begin{pmatrix} \mu_1 & 0 \\ 0 & \mu_2 \end{pmatrix} \begin{pmatrix} w_1 \\ w_2 \end{pmatrix} \quad (4)$$

where the eigenvalues are $\mu_1 \geq \mu_2 \geq 0$, and the eigenvectors are then $w_1 \parallel \nabla \vec{u}_\sigma$ and $w_2 \perp \nabla \vec{u}_\sigma$. Since μ_1 and μ_2 measure the variation of the color values within a neighborhood of scale $\mathcal{O}(\rho)$, they describe the average contrast in the eigendirections. Constant area are characterized by $\mu_1 \approx \mu_2 \approx 0$. Strong and straight edges give $\mu_1 \gg \mu_2 \approx 0$, and corners or less structured regions give $\mu_1 \geq \mu_2 \gg 0$. Hence, it offers a good way to measure the local coherence. Different ways to combine μ_1 and μ_2 exist. Here $\Delta = \sqrt{\mu_1 + \mu_2}$ is used, which is more respectful with the corner points, in comparison with $\sqrt{\mu_1 - \mu_2}$ or $\sqrt{\mu_1}$, see [7] for more details. Finally D was defined as:

$$D(J_\rho(\nabla \vec{u}_\sigma)) = (w_1 | w_2) \begin{pmatrix} \lambda_1 & 0 \\ 0 & \lambda_2 \end{pmatrix} \begin{pmatrix} w_1 \\ w_2 \end{pmatrix} \quad (5)$$

where:

$$\lambda_1 = \begin{cases} \alpha \left(1 - \frac{\Delta^2}{s^2}\right) & \text{if } \Delta^2 \leq s^2 \text{ and } |\angle w_2| > \theta_{min} \\ 0 & \text{else} \end{cases} \quad (6)$$

$$\lambda_2 = \alpha \quad (7)$$

λ_1 defines the diffusion intensity along $\nabla \vec{u}_\sigma$, and λ_2 along the structure. The parameter s is called the coherence threshold. Above it, no diffusion occurs in $\nabla \vec{u}_\sigma$ direction, therefore not corrupting the edge. On the other hand, it always diffuses along the edge. θ_{min} represents the prior information on objects, that is scars are unidirectional, along a dimension of the image thanks to the fixed acquisition procedure.

Shock Filters: Shock filters are hyperbolic partial differential equations based filters which were first proposed by Rudin and Osher. Here a recent improved version of Remaki and Cheriet [8] is used, since it allows a good control and parametrization of the shock velocity. Roughly speaking, this filter creates a shock in the position of zero-crossing of second derivative of the image, along the color gradient direction. A velocity parameter a let control the speed of the shock. This shock filter is used to balance the smoothing drawback of anisotropic diffusion, and to enhance the scar along its contour. Here it is made color coherence dependant by the use of Δ with a Tukey biweight function. The model is:

$$\partial_t u = -a(\Delta)F(\partial_{\eta\eta}u, \partial_{\eta}u)u_{\eta} \quad (8)$$

where

$$a = \begin{cases} 1 - \exp(-(\Delta^2 - s^2)) & \text{if } \Delta^2 \geq s^2 \\ 0 & \text{else} \end{cases} \quad (9)$$

and $F(a, b) = \text{sign}(a) \cdot \text{sign}(b)$. (1) and (8) are eventually combined to get the general model :

$$\partial_t u = \alpha_d \cdot \text{div}[D\nabla u] - \alpha_c \cdot a(\Delta)F(\partial_{\eta\eta}u, \partial_{\eta}u)u_{\eta} \quad (10)$$

where α_c and α_d allows to control the importance of each filter.

2.3 Segmentation Algorithm

The segmentation algorithm was based on the core of the edge detector of Ruzon and Tomasi [9]. The main idea is the use of color distributions instead of simple intensity neighborhood. Combined with the use of Earth Mover's Distance (EMD)[10] to measure distance between color distributions, it gives an efficient way to exploit channels correlation. On each point, a local circular weighted window of pixels is concerned. The size of this window has to be related to the characteristic size of a scar edge which is constant. This disk is divided in two equal portions with a rotating diameter. The color distribution of each is computed, and then the EMD between them. This EMD distance is bounded by $[0, 1]$, and represents the minimal amount of work to go from one distribution to the other in the color space, which is an instance of the transportation problem. The maximum EMD indicates the most asymmetric configuration, hence the precise direction of the local scar edge in the $[0, \pi]$ interval. The value of this maximum gives the strength of this local edge. This is how it also called. The minimum EMD indicates from global point of view how asymmetric the local

structure is. A corner or a junction for example will produce a higher minimum EMD than a strong binary edge. This minimum is called the asymmetry.

2.4 Postprocessing Algorithm

Since the scars are often scattered, and also because we are looking for an automatic scheme that only give a scar contour, we cannot use the simple maximum value postprocessing of Ruzon and Tomasi[9]. We have to process the segmentation algorithm outputs. Three measures are saved during the segmentation algorithm for every pixel of the image: the strength of the local edge, its orientation, and its asymmetry. These maps feed a K-means classification algorithm[11] with $K = 3$ classes: the scar, the background, the dermatoscopic stains.

Ideally the first class has no or few left stains. In practice, oblique and perpendicular stains, and also regular stains are very well eliminated thanks to the orientation measure and the fact that the scar is mainly unidirectional, and also the asymmetry measure. Unfortunately small irregular stains are often still present in the scar class. Therefore a second algorithm had to be designed in order to eliminate the most difficult stain. This algorithm is strongly designed for scars. It is based on an iterative study of perpendicular window histograms. From $i = 1$ to n (n is fixed by the length of the image), i windows are studied, and the histogram of each is calculated. See figure 2 for an example of windows cutting.

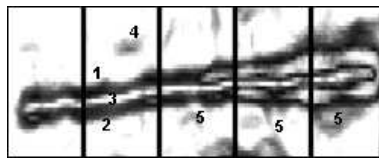


Fig. 2. The windows for the iterative histogram algorithm. $i = 5$

The model of a scar histogram and its possible stains is given on figure 3. Regions numbered on figure 2 referred to portions of the histogram of the figure 3. The region number 3 is quite interesting, and every time it can be detected, its position on the image is saved and will be reused in the spline approximation further. Two parameters are used during this step: τ_x which is related to the nominal width of a scar, and τ_m which is related to the nominal height of the scar histogram extrema versus the stains. Basically, with this two parameters - fixed for all scars - stains are detected and rejected of the image. The iterative concept helps to first eliminate the biggest stains, and increasingly reject smaller and closer to the scar stains.

Next, in order to split up the two parts of the scar, a smoothed approximation spline is calculated, using the positions of the regions numbered 3 in the iterative

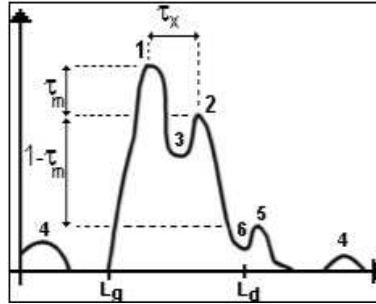


Fig. 3. The histogram model. Portions of the histogram on figure 3 refers to regions numbered on the figure 2

histogram algorithm. Then, each side of the scar is modelled with a weighted regression spline, whose smoothing parameter and coefficients are calculated with generalized cross-validation [12]. This fully automatic technique allows smooth regression without prior information on the signal and noise, and with very flexible conditions. For instance, the signal has not to be equally spaced. This proprieties of generalized cross-validation is useful here, since scar are often scattered, and since we do not have information on actual noise.

3 Results and Discussion

The algorithm has been tested on real patient images from St-Justine Hospital. One example of the pre-processing algorithm impact is given on figure 4. We can see that it preserves efficiently the scar while making the background more homogenous, and also improving the contrast. Details of three different scars enhancement are visible on figure 5.

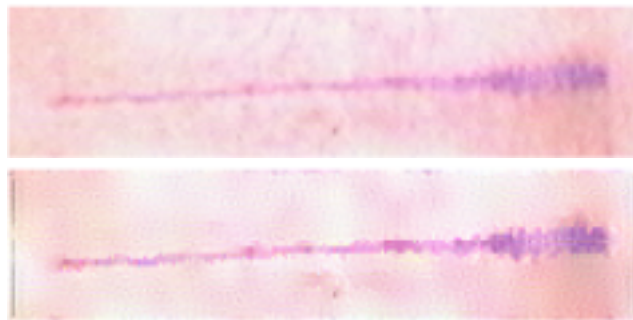


Fig. 4. An example of original and pre-processed images

On left and right scars, contrast enhancement on scar contour is quite obvious, such as the background denoising. In the middle, three big stains are fairly diminished, though not totally eliminated.

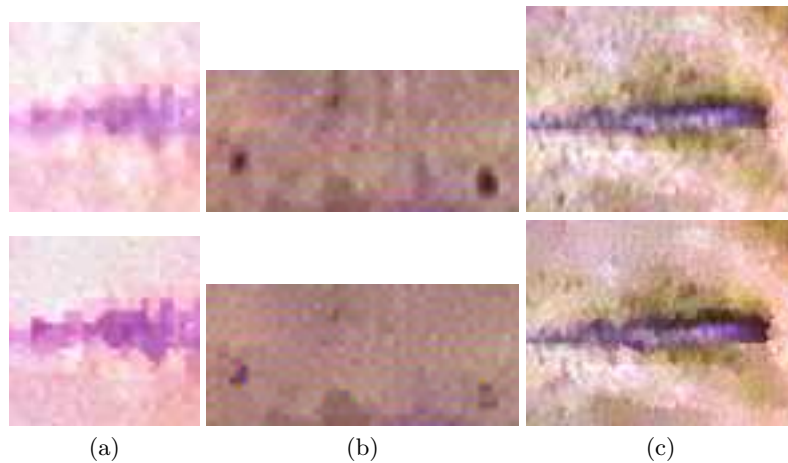


Fig. 5. Details of three scars, before (top) and after (bottom) the preprocessing filtering

On figure 6, the regions where a shock is created and its intensity. We see here that the filter is very selective and succeed in applying its wanted effect only on the object we want to enhance and further analyze. If shocks were uniformly created on the image, the background noise would be enhanced. Here diffusion and shock processes balance their own drawback very well. An example of the segmentation algorithm strength output is given on figure 7. Notice how the scar is quite scattered, and thus a simple maxima research would give open edges.



Fig. 6. Example of regions where a shock is created, i.e. where the contours are enhanced

On figure 8, three examples of extracted contours (blue) compared to those manually drawn by two different human operators on original images (green

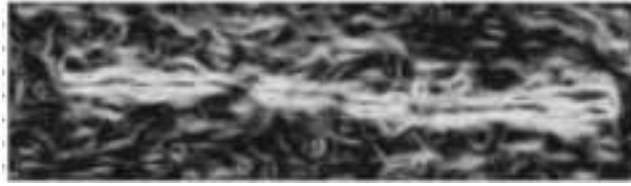


Fig. 7. An example of the segmentation algorithm strength output

and red). Notice that the vertical scale is bigger than the horizontal scale, to help the reader to see the performance between automatic and manual contours. The results demonstrated that average deviation between the manual contours and the automatic contour is $0.67 \pm 0.24 \text{ mm}$, which a very encouraging result knowing the resolution of the cameras (1.8 mm), and also noticing that the deviation between the two operators is $0.75 \pm 0.21 \text{ mm}$.

4 Conclusion

The segmentation scheme proposed in this paper is the first one that have been proposed for the segmentation of scar images, though this idea has been brought by the clinical department itself. The results obtained with the segmentation scheme proposed in this paper have been visually assessed by a trained nurse, and are promising for less than one year old scars. One major future work that is in progress is the use of the 3D information to evaluate the depth of the scar, and an objective validation using some clinical indices on a large group of scar images.

References

1. Philippe Schmidt, "Segmentation of digitized dermatoscopic images by two-dimensional color clustering," *IEEE Trans. Medical Imaging*, vol. 18, pp. 164–171, Feb 1999.
2. D.H. Chung, G. Sapiro, "Segmenting skin lesions with partial-differential-equations-based image processing algorithms," *IEEE Trans. Medical Imaging*, vol. 19, pp. 763–767, July 2000.
3. Valerie Pazos, Farida Cheriet, Hubert Labelle, Jean Dansereau, "3D reconstruction and analysis of the whole trunk surface for non-invasive follow-up of scoliotic deformities," *Research into spinal deformities, IOS Press*, vol. 4, 2002.
4. P. Perona, J. Malik, "Scale space and edge detection using anisotropic diffusion," *IEEE Trans. Pattern Anal. Machine Intell.*, vol. 12, pp. 629–639, 1990.
5. J. Weickert, "Coherence-enhancing diffusion filtering," *Int. J. of Comp. Vision*, vol. 31, pp. 111–127, 1999.
6. J. Weickert, "Coherence-enhancing diffusion of colour images," *Proc. VII National Symposium on Pattern Recognition and Image Anal.*, vol. 1, pp. 239–244, April 1997.

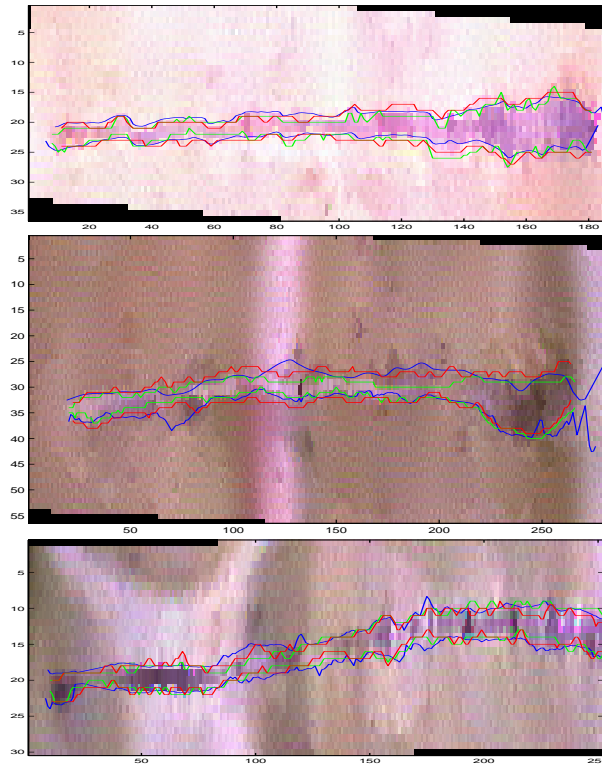


Fig. 8. Example of extracted contours (blue), compared with manually drawn contours by two different operators (green and red)

7. D. Tschumperle, R. Deriche, "Restauration d'images vectorielles par EDP," *RFIA Proc.*, 2000.
8. L. Remaki, M. Cheriet, "Numerical schemes of shock filter models for image enhancement and restoration," *Journal of Mathematical Imaging and Vision*, vol. 2, pp. 129–143, 2003.
9. M. Ruzon, C. Tomasi, "Edge, junction, and corner detection using color distributions," *IEEE Trans. Pattern. Anal. Machine Intell.*, vol. 23, pp. 1281–1295, Nov 2001.
10. Y. Rubner, C. Tomasi, L.J. Guibas, "A metric for distributions with applications to image databases," *IEEE Int. Conf. on Comp. Vision*, pp. 59–66, Jan 1998.
11. R.O. Duda, P.E. Hart, D.G. Stork, *Pattern Classification, second ed.* Wiley-Interscience, 2001.
12. P. Craven, G. Wahba, "Smoothing noisy data with spline functions," *Numerische Mathematik, Springer Verlag*, vol. 31, pp. 377–403, 1979.